Cell Tissue Res (2002) 309:301–311
DOI 10.1007/s00441-002-0559-2

REGULAR ARTICLE

Jochen Neuhaus · Hartwig Wolburg
Thomas Hermsdorf · Jens-Uwe Stolzenburg
Wolfgang Dorschner

Detrusor smooth muscle cells of the guinea-pig are functionally coupled via gap junctions in situ and in cell culture

Received: 26 October 2001 / Accepted: 22 March 2002 / Published online: 29 June 2002

Abstract Intercellular communication between smooth muscle cells is crucial for contractile behaviour in normal and pathologically altered urinary bladder. Since the study of coupling is difficult in situ, we established cell cultures of bladder smooth muscle cells to analyse coupling mechanisms. Microinjection of Lucifer yellow demonstrated syncytia composed of only a few to several dozen cells. Electron-microscopic examination of freeze-fracture specimens and ultrathin sections revealed that the dye-coupling was based on typical gap junction formation between the cultured smooth muscle cells. Furthermore, we were able to demonstrate gap junctions within the tissue fragments from which the primary cultures were grown. By Western blotting, we found connexin-43-positive protein bands both in native tissue probes from the guinea-pig urinary bladder and in smooth muscle cell cultures. Extracellular electrical stimulation of single cells evoked calcium transients, as visualized by fura-2 ratiofluorimetry. Calcium waves propagated throughout the syncytia with a declining amplitude, showing that the calcium signal was not regenerative. Therefore, the calcium signal was probably transmitted by a diffusible factor. These findings correlated well with the dye-coupling that we found between detrusor smooth muscle cells in situ. The use of smooth muscle cell cultures therefore seems to be a feasible approach for studying coupling behaviour in vitro.

This work was supported by a grant from the Deutsche Forschungsgemeinschaft, DFG, NE 425/4–1

J. Neuhaus (✉) · J.-U. Stolzenburg · W. Dorschner
Clinic for Urology, University of Leipzig, Stephanstrasse 11,
04103 Leipzig, Germany
e-mail: neuj@medizin.uni-leipzig.de
Tel.: +49-341-9719043, Fax: +49-341-9719009

H. Wolburg
Department of Pathology, University of Tübingen,
72076 Tübingen, Germany

T. Hermsdorf
Institute of Biochemistry, University of Leipzig,
04103 Leipzig, Germany

Keywords Dye-coupling · Calcium imaging · Electron microscopy · Freeze-fracture · Western blotting · Guinea-pig (male)

Introduction

Dysfunction or dysenergia of smooth muscles within the lower urinary tract is a common feature in urological diseases. Concerning the basic mechanisms of those disturbances, strong evidence has accumulated for a myogenic origin for the overactive and instable bladder (Brading 1997; Fry and Wu 1998). Electrical coupling between smooth muscle cells has been proposed to be a major component in all kinds of detrusor instabilities resulting in spontaneous pressure rises (Brading 1997). These instabilities often develop with ageing and it is not surprising that the ultrastructure of the detrusor smooth muscle is significantly changed in hyperactive bladders (Elbadawi et al. 1993) and in hypocontractile and obstructed detrusor (Hailemariam et al. 1997). The ultrastructural changes correlate well with urodynamic findings and are distinct for the clinically defined disorders. Of especially interest is the finding of an increase in ultra-close abutments and abundant so-called protrusion junctions in instable hyperactive detrusor. Protrusion junctions and ultra-close abutments both are characterised by narrowing of the extracellular space. In the case of the protrusion junction, the cell membranes approach up to 12 nm and less, but there is still some electron-dense material between them. At ultra-close abutments, there is no visible cleft left and therefore they are believed to represent true gap junctional contacts (Elbadawi et al. 1993). However, because of technical problems, gap junctions have not been positively identified within detrusor smooth muscle as yet.

Since it is technically difficult to study coupling behaviour in situ, we have developed a cell culture system for smooth muscle cells from lower urinary tract (Neuhaus et al. 2000). Electrical coupling has been analysed in various cultured smooth muscle cells by using patch clamp, calcium imaging techniques or dye-coupling (Young et al.

1996; Miyoshi et al. 1996; Little et al. 1995; Kimura et al. 1995; Watts et al. 1994). Coupling between cultured smooth muscle cells of the lower urinary tract, however, has not yet been demonstrated and analysed. To the best of our knowledge, this is the first report of the functional coupling of cultured smooth muscle cells from the lower urinary tract.

The guinea-pig has been used in this study, because the anatomical structures of this species are largely comparable to those of humans. In both species, the three individual layers of the detrusor (internal longitudinal layer, circular layer, external longitudinal layer) are the main directions of an otherwise densely interwoven muscle system. The musculature around the ostium urethrae internum forms an independent muscular unit, viz. the musculus sphincter vesicae (Neuhaus et al. 2001; Dorschner et al. 2001). As in the human, part of the pelvic nerve plexus is located within the muscular wall of the guinea-pig urinary bladder, thus providing the substrate for comparable local control of smooth muscle activity in the bladder and the bladder neck.

Here we present data demonstrating that the smooth muscle cells of guinea-pig detrusor are coupled in situ and form syncytia of various sizes in culture. We also show that the structural basis of coupling is the formation of classical gap junctions by connexin-43.

Materials and methods

Cell cultures

Male guinea-pigs of 350–550 g were sacrificed (intrapulmonary injection of 1 ml/kg T61; Hoechst) according to the guidelines of the local committee of animal care and use. The bladder was excised and transferred to a laminar-flow sterile working bench. Primary cell cultures were set up from fragments of the guinea-pig urinary bladder. The bladder was cut into two parts, the bladder dome and the bladder outlet, and cultures were initiated from these two regions separately. After removal of the mucosa, small tissue fragments of about 0.5×0.5×0.5 mm were plated onto tissue culture dishes (Greiner) covered with collagen A (Sigma-Aldrich, Germany). After 6 days in vitro (DIV), small colonies of smooth muscle cells had formed around the fragments. When kept in DMEM supplimented with 10% fetal calf serum at 37°C and 5% CO_2, the cultures grew to 70% confluence in about 14 DIV. All experiments reported here were carried out on these primary fragment cultures.

Immunocytochemistry

Selected cell cultures were immunocytochemically characterized. We used monoclonal antibodies against α-smooth muscle actin (1:2000, Sigma, Germany), calponin (1:1000, Sigma), desmin (Zymed Laboratories, USA; ready to use), smooth muscle myosin (1:600, Sigma) and vimentin (Zymed; ready to use) in combination with biotinylated secondary anti-mouse antibody and peroxidase staining and then diaminobenzidine/H_2O_2 as the chromogen (LSAB-Kit, DAKO Diagnostika, Germany). In brief, cell cultures were washed three times in 0.1 M phosphate-buffered saline (PBS) pH 7.4, fixed with methanol at –20°C for 10 min, washed in 0.05 M TRIS-HCl buffer pH 7.6 and incubated in 3% H_2O_2 in 70% methanol for 10 min to block endogenous peroxidase activity. To demask antigenic sites, the cells were incubated in 0.32% dimethyl sulphoxide (DMSO), 0.08% Triton X-100 in 0.05 M TRIS-HCl for 5 min. Unspecific binding was blocked with 3% skimmed dry milk, 1% bovine serum albumin (BSA) in 0.05% Tween 20 in TRIS-HCl. The cells were then incubated with the primary antibodies at room temperature for 2 h. Detection and visualization were performed according to the protocol provided by DAKO. Cultures were examined and photographed on a Diaplan light microscope (LEICA, Germany).

Dye-coupling

Native bladder

Male guinea-pigs (600–900 g) were sacrificed as described above. The urinary bladder was dissected out and stored in ice-cold oxygenated Krebs-Ringer (pH 7.4) with 1.5 µM nicardipine (Sigma) to prevent muscle contractions. The urothelium, submucosa and adventitial coat were carefully removed. Smooth muscle cell bundles were then dissected out under a binocular microscope. Impalement of single muscle cells was achieved by using glass micropipettes of 25–60 MΩ resistance mounted on a micromanipulator. The pipettes were filled with 1% Lucifer yellow (LY, MW 457 Da; Sigma) in 0.1 M lithium-acetate and the cells were dialysed with LY by a hyperpolarizing current (0.5–3 nA) for 10–15 min. After the experiment, the nuclei of the cells were stained with 4,6-diamidino-2-phenylindole (DAPI; 1:5000; Hoechst, Germany), washed in 0.1 M/l PBS and covered in Permaflour (Immunotech, France).

Cultured smooth muscle cells

Single cells in 70%–100% confluent smooth muscle cell colonies or in native guinea-pig urinary bladder were dialysed for 10 min with 0.1%–3% LY dissolved in intracellular pipette solution (Klöckner and Isenberg 1985; 130 mM KCl, 5 mM K-pyruvate, 5 mM K-oxalacetate, 5 mM K-succinate, 10 mM HEPES, 0.02 mM EGTA adjusted to pH 7,4) by using a patch clamp micropipette (6–10 MΩ).

The LY-filled micropipette was pushed tightly against the surface of a cell. As soon as membrane resistance rose considerably, the cell membrane was sucked into the tip of the micropipette until the membrane broke and the cell started to dialyse. As seen in pilot experiments (data not shown), it was of no advantage to use constant hyperpolarizing current pulses. Some experiments were performed with 50 MΩ micropipettes for sharp penetration and LY was injected into the cell by short reproducible pressure pulses by using a PV800 Pneumatic PicoPump (World Precision Instruments, USA). The pressure and pulse length were adjusted, so that an efflux of LY was just visible under a fluorescence microscope at a magnification of 40×. The numbers of coupled cells were counted under a fluorescence microscope equipped with a filter set suitable for fluorescein isothiocyanate. Several cultures were fixed in PBS-buffered 4% paraformaldehyde pH 7.4 for 1 h at 4°C in the dark for immunocytochemical detection of LY. Endogenous peroxidase activity was blocked by incubating the cultures in 70% methanol with 3% H_2O_2 for 10 min. After a 5-min incubation in 0.32% DMSO, 0.08% Triton X-100 in 0.05 M TRIS, pH 7.6 (DT-TRIS), unspecific binding was blocked with 3% (w/v) nonfat dry milk, 1% (w/v) BSA, 0.05% Tween 20 in DT-TRIS. The polyclonal rabbit anti-LY antibody (Molecular Probes, USA) was diluted 1:500 in this blocking solution and the cells were incubated for 2 h at room temperature. For visualization, the DAKO LSAB peroxidase staining kit was used routinely with diaminobenzidine/H_2O_2 as chromogen. Cell nuclei were counterstained with Meyer's haematoxylin.

SDS polyacrylamide gel electrophoresis and Western blotting

The monolayers were rinsed three times with ice-cold PBS and scraped off in 1 ml PBS containing protease inhibitors (1 mM EDTA, 0.1 mM phenylmethanesulphonyl fluoride, 20 µM leupep-

tin, 10 µM antipain, 20 µM pepstatin). Harvested cells were centrifuged at 3000 *g* for 10 min at 4°C. The pellet was resuspended in 0.5 ml ice-cold PBS with protease inhibitors and homogenized by sonication (3×10 s). The protein concentration in homogenates was measured by the method of Bradford (Bradford 1976). Homogenates were precipitated by trichloroacetic acid (5% final concentration). After centrifugation, the protein pellets were dissolved by the addition of sample buffer (62.5 mM TRIS-HCl pH 6.8, 10% glycerol, 2% SDS, 0.7 M β-mercaptoethanol, 0.0025% bromphenol blue) and boiled for 10 min at 95°C. SDS polyacrylamide gel electrophoresis (SDS/PAGE) was performed by the method of Laemmli (1970) with 10% (w/v) polyacrylamide gels. Aliquots containing 50 µg protein were applied per lane. In order to determine the molecular weight, myosin (200 kDa), β-galactosidase (116.4 kDa), phosphorylase b (97.4 kDa), BSA (66.2 kDa) and aldolase (39.3 kDa) were used as standards. For Western blotting, proteins were transferred from unstained SDS gel to a polyvinylidene fluoride membrane by the TransBlot SemiDry System from Bio-Rad Laboratories (Germany) at 15 V for 30 min. Blocking of nonspecific binding was performed by incubating the membrane for 30 min in 5% nonfat dry milk, 0.5% BSA dissolved in PBS with 0.05% Tween-20. Incubation was carried out with a monoclonal anti-connexin-43 antibody (Zymed) for 1 h in PBS-Tween at room temperature. Unbound antibodies were removed by washing three times with PBS-Tween for 5 min. The membrane was then incubated for 1 h with anti-mouse-IgG-linked peroxidase (Boehringer Mannheim) followed by washing steps and colourizing with 3,3'-diaminobenzidine tetrahydrochloride/H_2O_2. To test the specificity of the reaction, the primary antibody was mixed with 10 µg/ml purified rat connexin-43 (Zymed) before incubation with the blot membrane according to the protocol of Zymed. The peptide was used to produce the anti-connexin-43 monoclonal antibody and corresponded to a cytoplasmic sequence located near the C-terminus of rat connexin-43 (Beyer et al. 1987; Fishman et al. 1990).

Electron microscopy

Cell cultures were washed three times in PBS at pH 7.4 before fixation in 2% glutaraldehyde in 0.1 M PBS for 1 h at 4°C. For ultrathin sectioning, the cells were postfixed in 1% buffered OsO_4, washed several times in PBS and dehydrated in a graded ethanol series. The 70% ethanol was saturated with uranyl acetate for contrast enhancement. The dehydrated cells were embedded in situ in Araldite (Serva, Germany) and sectioned on a Leica Ultracut R ultramicrotome. Ultrathin sections were stained with lead citrate for contrast enhancement. For freeze-fracturing, the glutaraldehyde-fixed cells were scraped off the culture dish, treated with 30% glycerol for 30 min and then placed between two gold specimen holders. After shock-freezing in a nitrogen slush at –210°C, the specimens were transferred into a Balzers freeze-fracturing apparatus (BFA 400 D, Balzers, Liechtenstein) and fractured at –150°C and 5×10^{-6} mbar (1 bar=10^5 Pa). The fracture faces were immediately shadowed with platinum/carbon (2 nm, 45°) and carbon (20 nm, 90°) for stabilization. The replicas were cleaned with 12% sodium hypochlorite, washed several times in double-distilled water and mounted on Pioloform-coated copper grids (Wacker Chemie, Germany). Ultrathin sections and replicas were observed in a Zeiss EM10 electron microscope.

Calcium imaging

The cells were incubated for 45 min with 2.5 µM/l fura-2-AM (Molecular Probes), the membrane-permeable acetoxymethyl ester of the calcium-sensitive fluorescent dye fura-2 (MW: 832 Da). When inside the cell, the ester is hydrolysed by endogenous esterases and the fura-2 accumulates within the cell. Fura-2 has various excitation maxima depending on the binding of calcium ions. Measurements of the intracellular calcium concentration are performed by acquiring two subsequent fluorescence images at 510 nm with an excitation of 340 nm (Ca^{2+} ions bound) and 380 nm (free fura-2). The ratio of the fluorescence measured for every single pixel and calculated according to the equation of Grynkiewicz et al. (1985) is directly proportional to the concentration of free calcium ions. By using the fluorescence intensity ratio for the calculation of the calcium concentration, bleaching and background noise can be substantially corrected.

After being thoroughly washed in Krebs-Ringer (in mM/l: NaCl 120.9, KCl 5.9, $NaHCO_3$ 14.4, $MgCl_2$ 1.2, $CaCl_2$ 2.5, NaH_2PO_4 1.2, glucose 11.5, HEPES 4.2) pH 7.2 at room temperature in the dark, the cell cultures were mounted on an upright fluorescence microscope (Axioskop FS, Carl Zeiss Microscopy, Germany) equipped with a Zeiss Achroplan 40×/0.80 water immersion objective and an Imago charge-coupled device camera attached to a personal computer. For acquisition of image sequences and to control the Polychrome II monochromator, TILLvisION v3.30 software (TILL Photonics) was used. Calculation of the kinetics and the calcium concentrations was performed after calibration of the system by means of the calcium calibration buffer kit no. 1 (Molecular Probes). For demonstration of functional syncytia, single cells within regions of 60%–100% confluence were stimulated by extracellular voltage jumps of –5 to –10 V for 25 ms with a Master-8 programmable pulse generator (AMPI, Israel). The micropipette was repositioned several times to stimulate different cells within the smooth muscle cell layer. During the experiment, the cell cultures were continously superfused with Krebs-Ringer at a flow rate of about 2 ml/min. All experiments were performed at 23–26°C (room temperature).

Calculations were carried out on original data as acquired with the Vision software package (TILL Photonics) by Microsoft Excel (Microsoft, USA). For calculation of time distances between the calcium response in different regions of interest (ROIs), a threshold of 125% of the base-line calcium level was used.

Results

Immunocytochemistry

Smooth muscle cells grew out of the fragments within 3 DIV and had formed small colonies around the fragments by 7 DIV (data not shown). Immunocytochemical analysis showed that 100% of the elongated cells stained intensely for the intermediate filament protein vimentin (Fig. 1B). Staining for the smooth muscle cell-specific markers, viz. smooth muscle cell α-actin and smooth muscle cell myosin heavy chain (SM1 and SM2), was less intense but, nevertheless, most cells were positive for these markers (Fig. 1C, D). For myosin, we observed a patchy staining pattern, with some colonies stained to about 60% and other colonies with only a few single cells being stained. The morphology in those colonies did not vary so that it was assumed that the expression of myosin heavy chain polypeptides was simply below the detection threshold. We used a monoclonal anti-desmin antibody directed against human desmin (57 kDa) showing no cross-reactivity to other filament types, including vimentin and cytokeratin. This antibody stained 100% of the elongated cells confirming their myogenic origin (Fig. 1E). Calponin is a 34-kDa calmodulin that binds to a specific site of the tropomyosin and is reported to be a very reliable, specific smooth muscle cell marker (Takahashi et al. 1988; Gimona et al. 1990). Calponin was detected with variable staining intensity in most of the cells resembling smooth muscle cells or myofibroblasts (Fig. 1F).

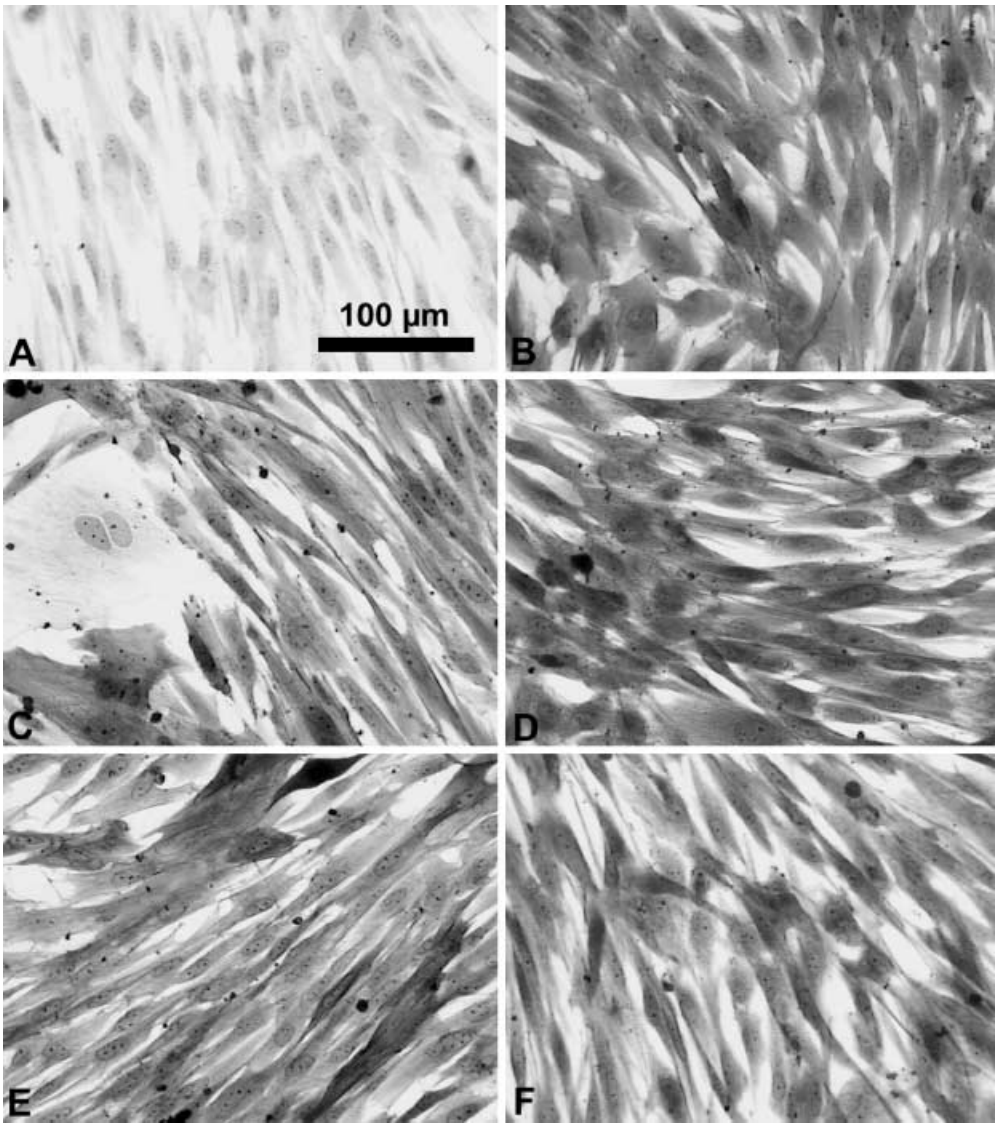

Fig. 1A–F Expression of various marker proteins in a culture from guinea-pig bladder dome at 12 DIV. For comparability of the staining intensities, the microscope illumination was adjusted to that of the control culture. The immunocytochemical stainings were aquired with excactly the same settings. **A** Control. **B** Vimentin. **C** Smooth muscle cell α-actin. **D** Smooth muscle cell myosin. **E** Desmin. **F** Calponin. Staining was very intense with the mesenchymal marker vimentin **(B)**. The smooth muscle cell-specific markers desmin and calponin stained most of the cells intensely, whereas α-smooth muscle cell actin and myosin staining was less prominent in this culture **(C, D)**

Dye-coupling in native guinea-pig urinary bladder in situ

All successful impalements of detrusor smooth mucle cells led to at least two stained cells. In most cases, three cells and, in one case, even four cells were coupled (Fig. 2). A mean of 2.64 (SD=0.58, *n*=22) smooth muscle cells were dye-coupled in the detrusor muscle. In all cases, the syncytia were oriented in line with a major smooth muscle cell bundle.

Dye-coupling in guinea-pig urinary bladder smooth muscle cells in culture

Dialysis of the cytoplasm of the impaled cell with LY occurred very rapidly (within several seconds; monitored in several experiments; data not shown). The diffusion of the dye throughout the syncytium was achieved within 10 min after successful impalement. Prolongation of the experimental time (up to 30 min) did not yield further labelled cells. The diffusion was fast enough to label syncytia of more than 100 cells within 10 min of dialysis. There was no obvious difference when using patch clamp technique or sharp electrodes. Since, in fragment cultures, the smooth muscle cells formed colonies around the tissue fragments (Fig. 3), regions of 70%–100% confluence were available for experiments over a wide time range (12–20 DIV). The borders of the syncytia were clearly demarcated, especially after the immunocytochemical detection of LY and processing for light microscopy. As demonstrated in Fig. 3, the number of dye-coupled cells varied from a few cells (arrowheads) to more than 100 cells; 23 experiments on primary fragment cultures from guinea-pig bladder gave a median of 14 with a range of a minimum of 1 to a maximum of 110 coupled cells. For an interpretation of the significance of the number of coupled cells, it must be taken into account that the degree of confluence varied considerably in different experiments. However, even in cases when the cells were not densely packed, several

cells were usually dye-coupled and showed dot-like contacts (Fig. 3 inset, arrows). The largest syncytia were observed in regions where the cells had formed multilayers. We regularly observed differences in staining intensity within the cells of one syncytium. This effect did not depend on the distance of the coupled cells from the impaled cell, so that we concluded that there were differences either in the number or in the opening state of the gap junctions. The observation that even a few dot-like contacts between cells can yield intensive staining of the neighbouring cell speaks in favour of gap-junctional conduction properties being regulated.

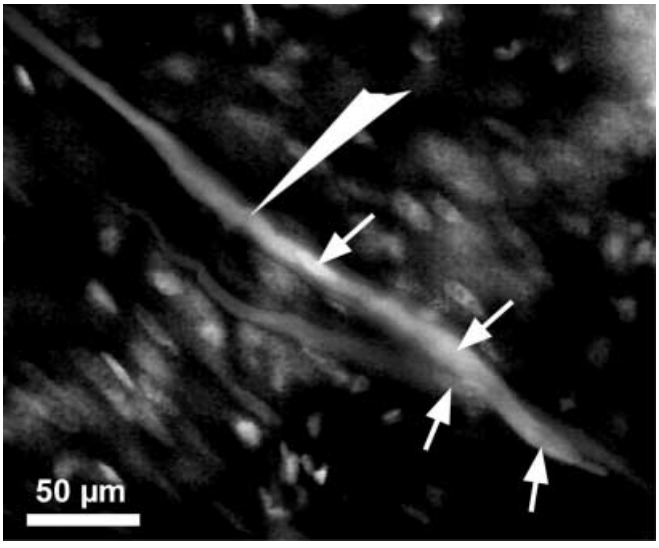

Fig. 2 Dye-coupling between detrusor smooth muscle cells (*large arrowhead* site of impalement, *arrows* nuclei of the coupled cells). The image was composed electronically by superimposing LY-fluorescence (*green*) with DAPI-fluorescence (*blue*). Note three aligned cells, with one cell lying slightly obliquely. This cell was clearly located underneath the others

SDS/PAGE and Western blotting

Two connexin subtypes were compared for their expression in cell cultures and in native bladder. Cell cultures were grown from the bladder dome and from bladder base, whereas probes from native bladder were taken from the corresponding regions, viz. the bladder dome and bladder base. For a positive control, guinea-pig heart muscle cells were used. Connexin-43 immunoreactivity was found regularly in guinea-pig bladder and heart and in cell cultures from guinea-pig bladder. Expression of connexin-43 varied considerably within the cell cultures. The most prominent protein band was indeed found in cell cultures from the bladder base, whereas the probes from bladder (whole organ) and heart were comparable in intensity (Fig. 4). To test for specificity, the anti-connexin-43 antibody was mixed with purified connexin-43 peptide (10 µg/ml); this resulted in the almost complete blockage of staining (Fig. 5, lanes 4, 5). The Western

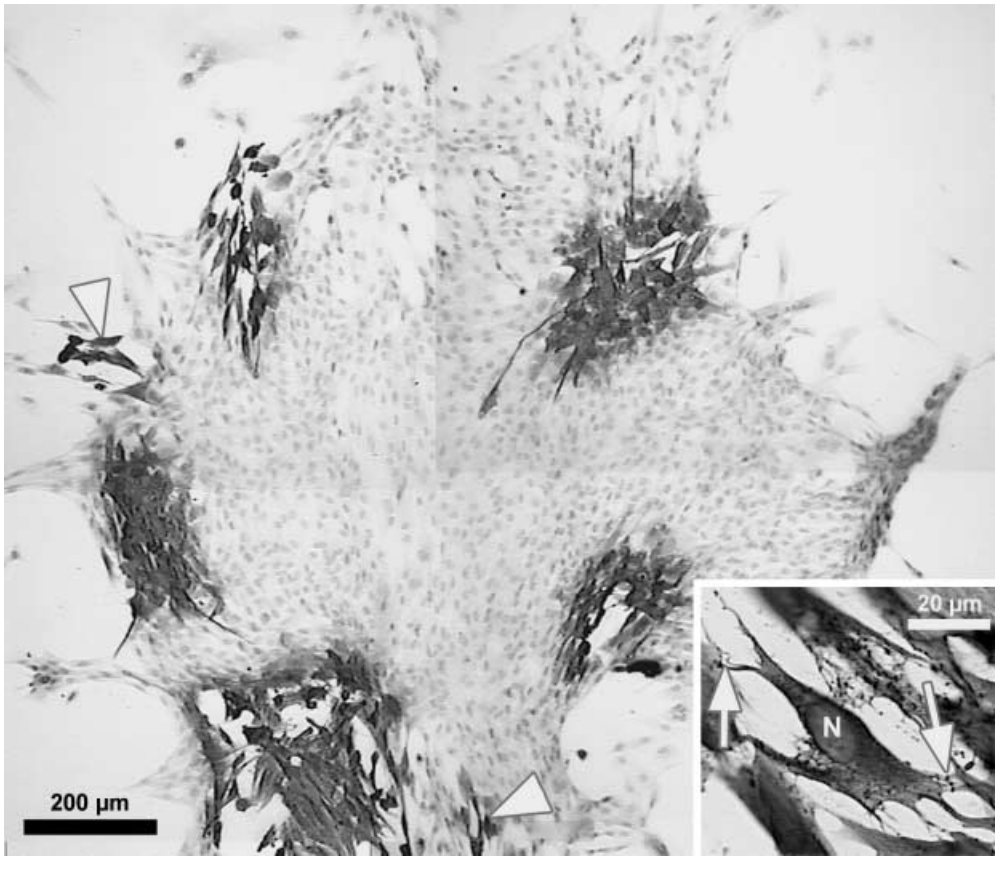

Fig. 3 Dye-coupling in cultured smooth muscle cells. Low magnification of a colony from guinea-pig detrusor, 12 DIV. Several dye-coupling experiments were performed. The duration of each LY injection was 10 min. LY was converted by immunocytochemical procedure to a brown precipitate that could be observed by light microscopy. Note the variation in the size of the syncytia with some consisting of only few cells (*arrowheads*), whereas others are formed by large numbers of cells. *Inset*: At higher magnification, the formation of dot-like contacts between single cells within the syncytium can be seen (*arrows*). Note that the staining intensity is high in this cell (*N* nucleus) although the junctional area is small

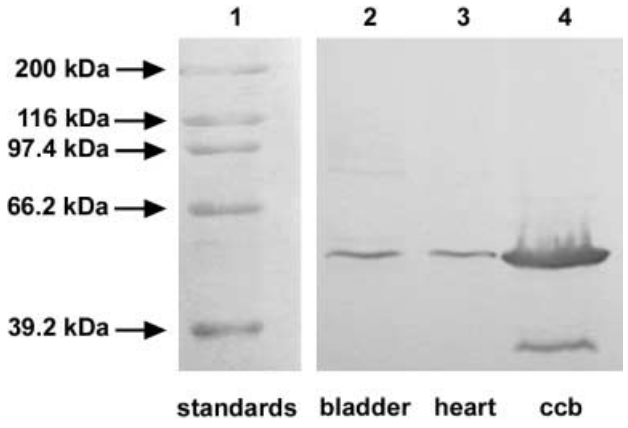

Fig. 4 Western blot analysis of connexin-43 expression in guinea-pig bladder, heart and cell cultures from bladder base (*ccb*). *Lane 1* Molecular weight standard stained with Coomassie blue, *lane 2* bladder, *lane 3* heart, *lane 4* ccb. In all samples the protein amount used was 50 µg. Note the prominent protein band at 56 kDa in *lane 4*. Cell cultures regularly show an additional protein band at about 35–39 kDa (*lane 4*)

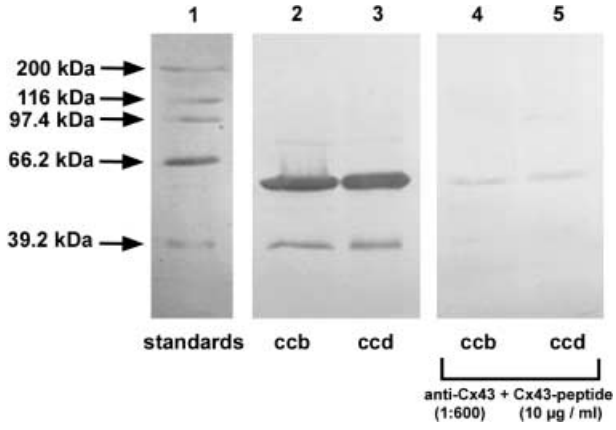

Fig. 5 Specificity of connexin-43 antibody staining. In cell cultures from bladder base (*ccb*) and bladder dome (*ccd*), incubation with connexin-43 peptide (10 µg/ml) almost completely blocked the 56-kDa band (*lanes 4, 5*) and abolished the 39-kDa band

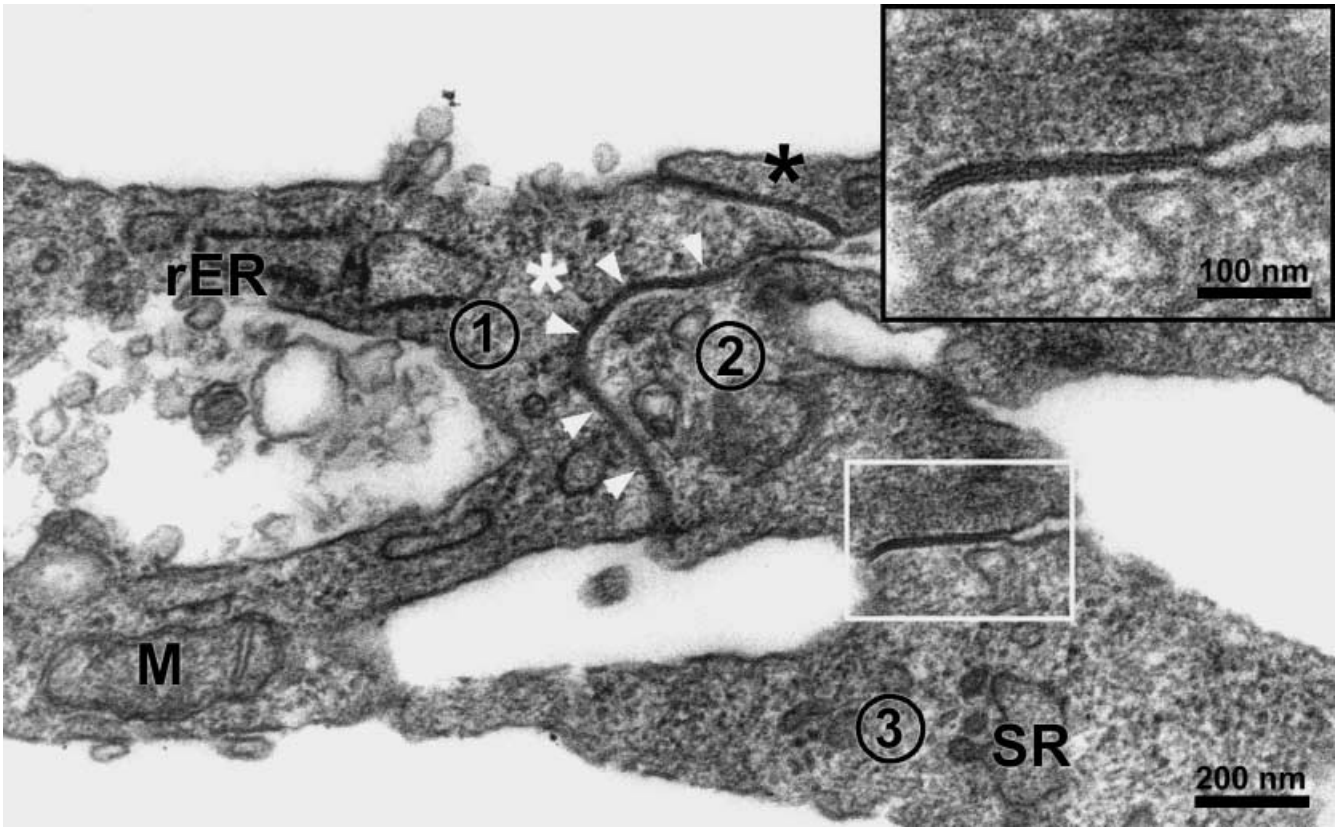

Fig. 6 Smooth muscle cell culture from guinea-pig bladder dome forming a multilayer. Three cells (numbered *1–3*) are interconnected by gap junctions (*arrowheads* course of a gap junction). Gap junctions were located at cell protrusions (*black asterisk*) and invaginations (*white asterisk*), respectively. Ultrathin section (*M* mitochondrion, *rER* rough endoplasmic reticulum, *SR* sarcoplasmic reticulum). *Inset*: Higher magnification of one of the gap junctions (*boxed*)

blot showed two distinct protein bands at 56 kDa and at about 35–39 kDa. The slight protein band of lower molecular weight was possibly a proteolytic product of the 56-kDa protein. The 56-kDa band occurred in all positive smooth muscle cell samples and in heart. All experiments were repeated at least twice with different cell cultures and tissue probes. From these experiments, it became clear that the expression of connexin-43 was variable in cultured cells.

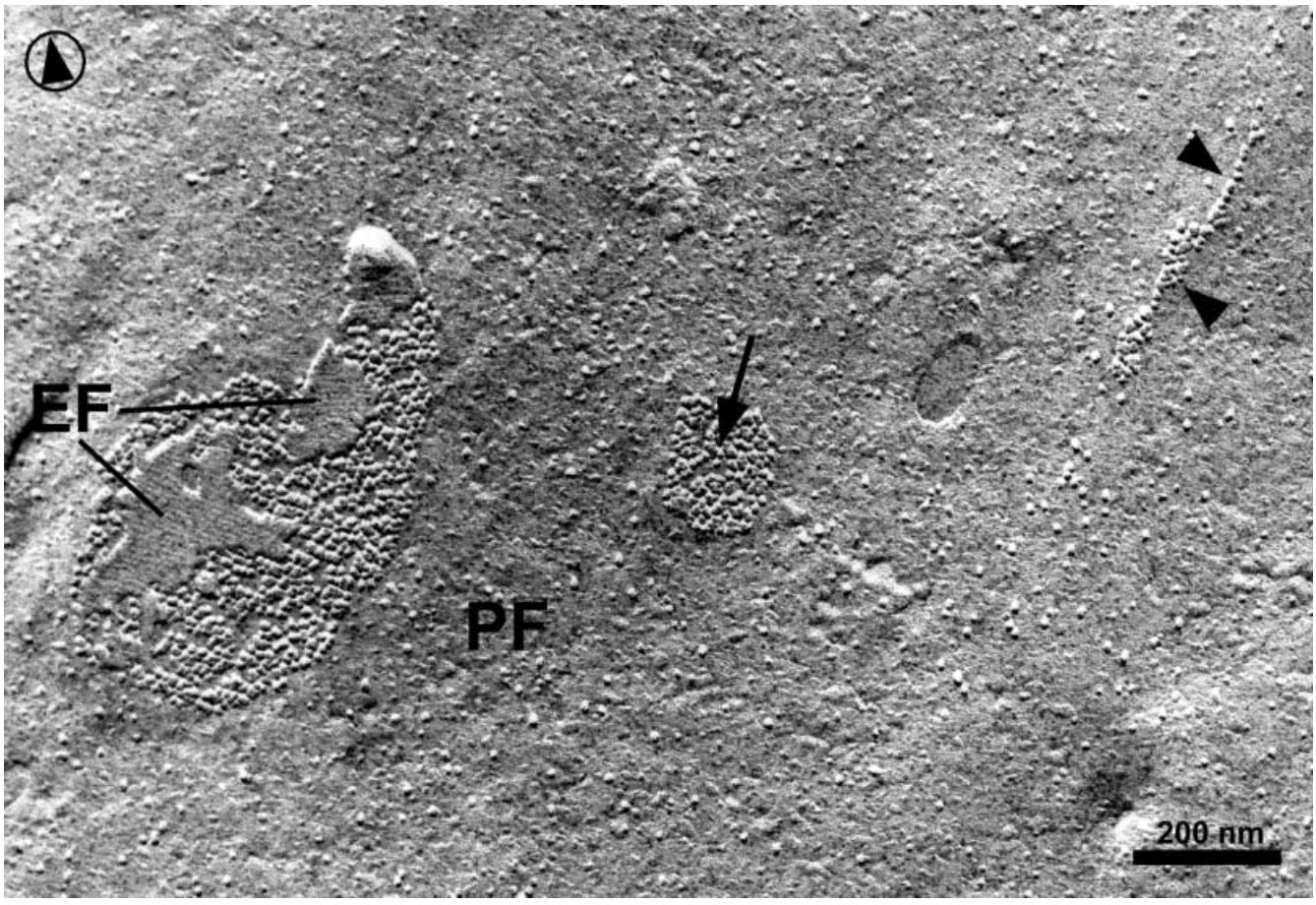

Fig. 7 Freeze-fracture replica of a smooth muscle cell, cultured from guinea-pig bladder dome. Numerous intramembranous particles (IMPs) of various sizes are visible on the protoplasmic fracture face (*PF*). Some IMPs, 8–9 nm in diameter, are clustered (*arrows*) forming typical gap junction patches. Some of them are lined up forming a thread (*arrowhead*). The extraplasmic fracture face (*EF*) shows the typical gap junction pits (*encircled arrowhead* shadowing direction)

Electron microscopy

Ultrathin sections clearly demonstrated the multilayered growing pattern of cultured smooth muscle cells (Fig. 6). In these regions, cell protrusions closely approached the neighbouring cell, often forming interdigitated contact zones with typical gap junctions (Fig. 6). In contrast, gap junctions were rarely found in the perinuclear regions. Although the cells formed a three-dimensional structure, the intercellular space between the cells was usually larger than that in situ (see later) restricting the direct cellular contact to the periphery of the cell. Unlike the situation in situ, there were no intermediate junctions seen in cell culture; neither were dense band patterns found underneath the plasma membrane of cultured smooth muscle cells.

In freeze-fracture preparations, we found typical gap junctions formed from particles of 8–9 nm, associated with the protoplasmic fracture face (PF) and leaving pits on the extraplasmic fracture face (EF). The arrangement of the single connexons differed, causing variously sized patches of connexons and sometimes strings of particles (Fig. 7). Except for the occurrence of gap junctions, the fracture faces showed no special intramembranous particle formations. No tight junctions were found.

The morphology of cultured smooth muscle cells differed in many aspects from the smooth muscle cells found in native detrusor muscle (Fig. 8). The cells had a dense cytoplasm with abundant filaments, rough and smooth endoplasmic reticulum (sarcoplasmic reticulum) and mitochondria (Fig. 8). Microtubules, pinocytotic vesicles and coated pits were seldom found. Intermediate filament content was low compared with the contractile type of smooth muscle cells in situ (Figs. 6, 8). No gap junctions could be detected in ultrathin sections or in freeze-fracture preparations of the native guinea-pig detrusor. However, numerous junctions were present with an intercellular distance of about 30 nm, electron-dense material underneath the plasma membrane and a dense lamella in between (Fig. 8B, arrows). We never observed such a type of junction in cell culture.

Calcium imaging

Because of technical problems, calcium imaging experiments were performed solely on cultured cells. Cells

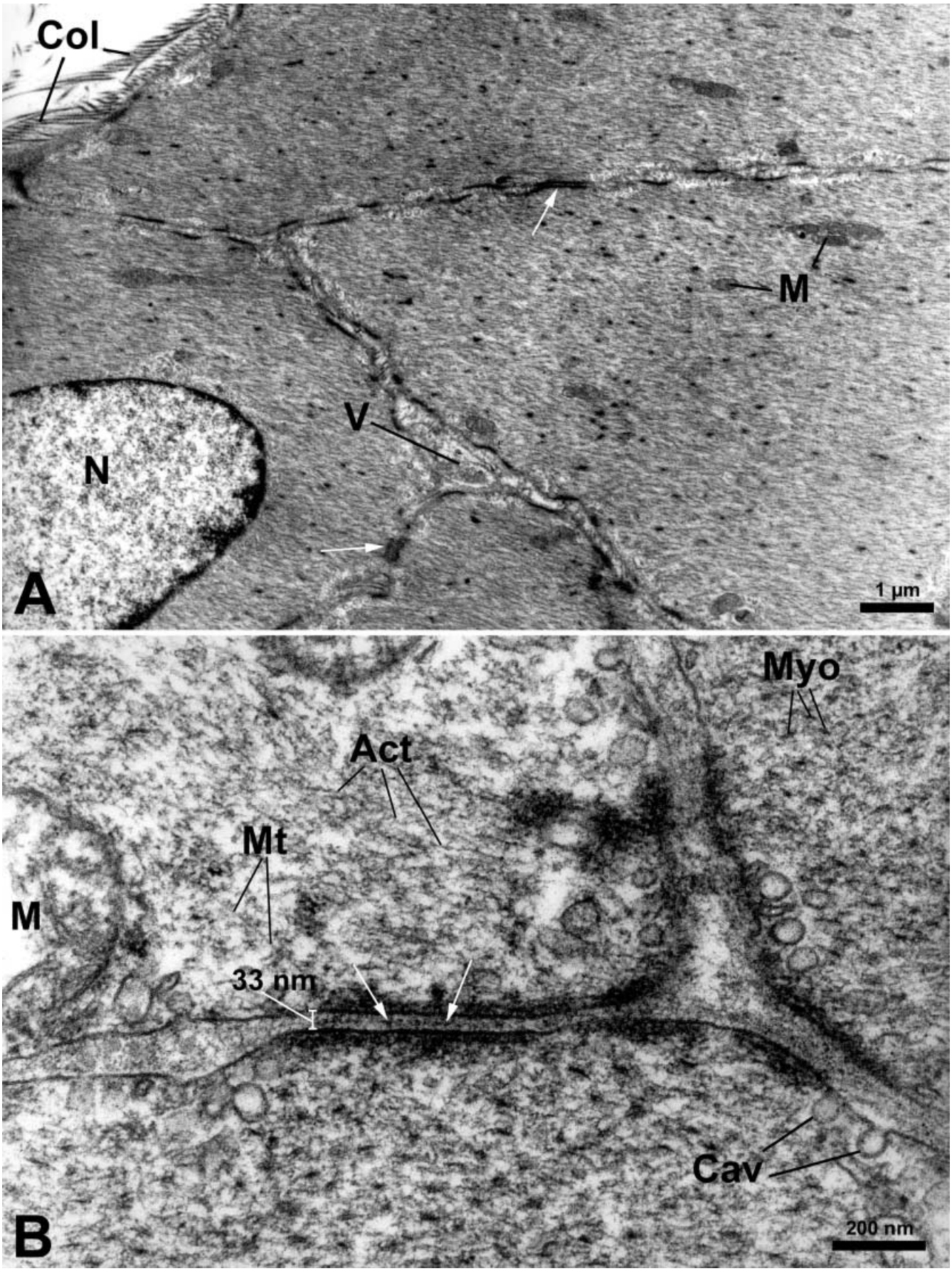
Col
M
V
N
A
1 µm
Myo
Act
Mt
M
33 nm
Cav
B
200 nm

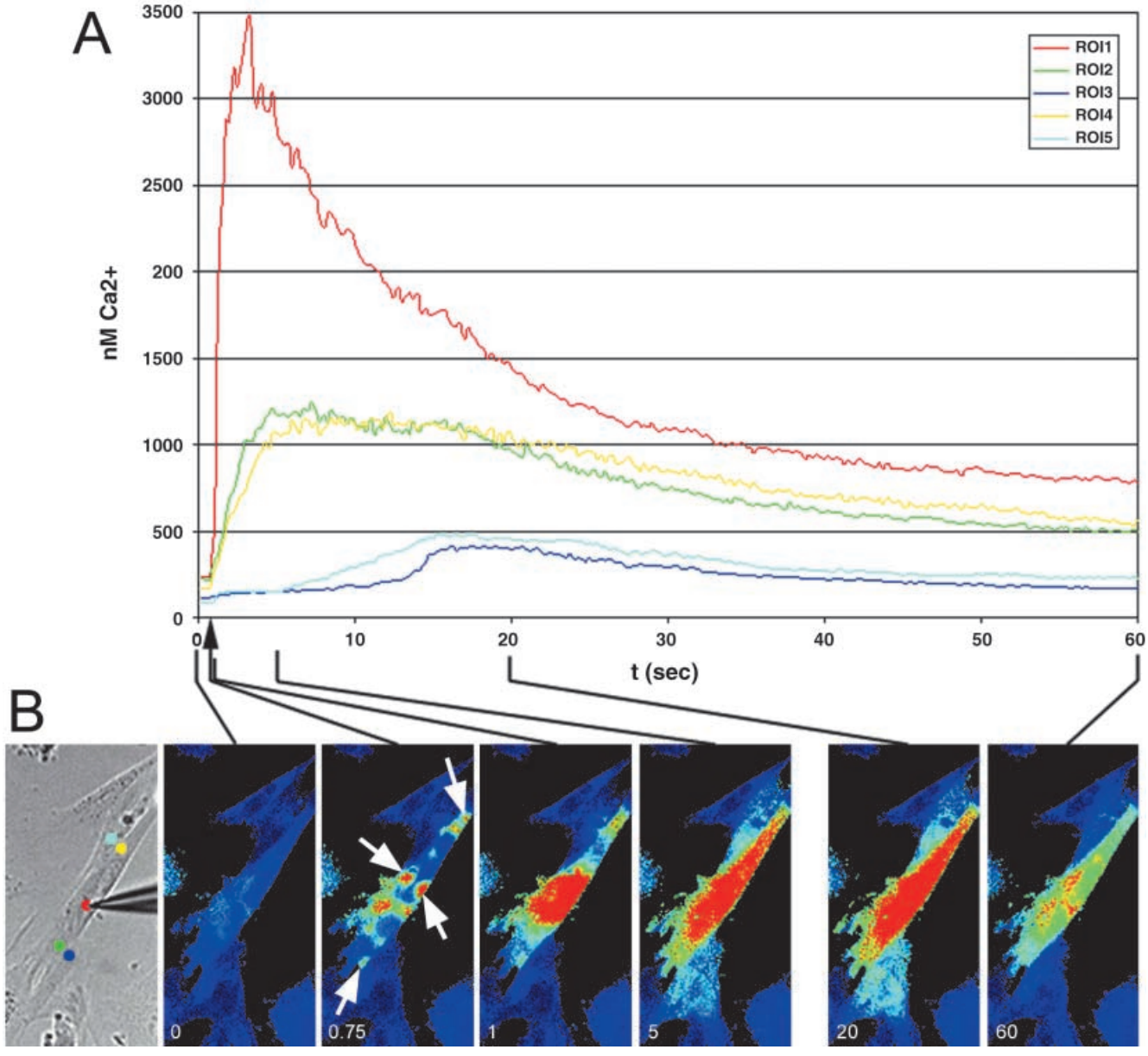

Fig. 9A, B Calcium wave in cultured detrusor smooth muscle cells. Marks in **B** correspond to the colours of the kinetics in **A** taken as an average from the marked regions of interest. *Numbers* in *coloured images* in **B** give the time point of the measurement in seconds. In phase-contrast image, the location of the stimulation micropipette is just *above* the marked *red* region. This cell was extracellularly stimulated by a short depolarizing voltage jump (–5 V, 25 ms). Immediately upon stimulus application, the intracellular Ca^{2+} concentration rose steeply (**A**, *red line*). The occurrence of hot spots even at remote areas of the cell membrane indicates that the signal was probably spread electrotonically over the cell membrane (**B**, 0.75). Thus, the Ca^{2+}-rise in the *green* and *yellow* region was almost synchronous (**A**). The signal was significantly delayed at the cell border and the velocity of the calcium wave was about 1 µm/s at the cell-cell contact

◀ **Fig. 8** Electron micrographs of ultrathin sections of guinea-pig detrusor muscle. **A** Smooth muscle cells lie closely together and are interconnected by special cell-cell contacts (*arrows*). There are no obvious interdigitations. Varicosities (*V*) can occasionally be seen between the cells (*M* mitochondrion, *N* nucleus, *Col* collagen). **B** Smooth muscle cells show regularly distributed myosin (*Myo*) and actin (*Act*) filaments. Only a few microtubules are visible (*Mt*). The plasma membrane shows numerous caveolae (*Cav*). The intercellular space is about 100 nm wide and narrows to about 30 nm within the junctional region. The intermediate junctions are characterized by electron-dense material underneath the plasma membrane with a middle lamella in the extracellular space (*arrows*)

were loaded with fura-2 as described above. When stimulating single cells within the smooth muscle cell layer with extracellular voltage jumps (–5 V, 25 ms), we found that 14% (n=69) of the stimulated cells did not show any calcium elevation, whereas 30% of the cells showed a moderate, 26% a good and 29% a strong elevation of the calcium concentration in semiquantitative analysis (ranking: 0–3). Of the cells, 29% were not coupled to another cell. The mean number of coupled cells was 2.68 (SD=2.26, n=59).

The calcium wave evoked by the stimulation travelled with decreasing amplitude throughout the functional syncytium (Fig. 9). The velocity of the calcium wave varied from 1 µm/s to 26 µm/s with a mean velocity of 8±6.38 µm/s (*n*=31). As illustrated in Fig. 9, the intracellular spread of the calcium signal was fast and could not be resolved by the acquisition time of 250 ms used in this experiment. The patchy appearance of "hot spots" even in distant regions of the cell (Fig. 9, at 0.75 s, arrows) favoured the notion that, in this particular experiment, the electrical signal spread electrotonically over the cell membrane causing almost synchronous calcium elevations at various sites of the cell. The delay of calcium elevation was 13 s (ROI2/ROI3) and 8 s (ROI4/ROI5), respectively. These delays corresponded to a velocity of the calcium wave of about 1 µm/s at the cell-cell contact site. Since the intracellular spreading of the calcium wave was so rapid, the observed delay of the calcium signal rising from one cell to another was probably mainly caused by the delay at the gap junction. From stimulation experiments (n=31), we calculated a mean spreading velocity of 8±6.38 µm/s (mean±SD).

Discussion

Gap-junction-mediated communication between smooth muscle cells is believed to play a major role in normal and altered systems. In vascular smooth muscle cells, there is good evidence that coupling is an important factor in the modulation of the vasomotor tone (for reviews, see Christ et al. 1996; Brink 1998). As reviewed by Hanani and Brading (2000), electrical coupling between smooth muscle cells seems to be an universal feature of all smooth muscle cells.

We have been able to demonstrate dye-coupling and functional coupling between smooth muscle cells of the guinea-pig detrusor in situ and in cultured smooth muscle cells. There are only a few reports on the coupling properties of guinea-pig detrusor smooth muscle cells in the literature. Fry et al. (1999) have measured electrical impedance of guinea-pig detrusor smooth muscle strips and compared the intercellular resistance with that of the myocardium. They have found that the gap junction resistance is larger in detrusor than in myocardium but have nevertheless concluded that detrusor smooth muscle cells are well coupled because of the high membrane resistance. Hashitani et al. (2001) have studied the propagation of spontaneous excitation in the smooth muscle of the guinea-pig urinary bladder in situ and shown by injection of neurobiotin that this gap junction permeable molecule spreads into three to five neighbouring cells in the axial direction. This is in good agreement with our own in situ dye-coupling experiments on native guinea-pig urinary bladder (mean = 2.6 coupled cells) with LY, which has a higher molecular weight (MW 457 Da vs MW 367 Da) and therefore diffuses less readily. As demonstrated by Western blot analysis, connexin-43 is found in considerable amounts in guinea-pig detrusor muscle. We therefore conclude that although we have not found any "classical gap junctions" in electron-microcopic preparations, the smooth muscle cells form gap-junction-like contacts. One possible explanation for not finding gap junctions could be that they solely occur at the protrusion contacts between the smooth muscle cells and that this region is rarely exposed in freeze-fracture preparations. On the other hand, it seems possible that no classical gap junctions are formed at all but that the connexons are located within the intermediate junctions. Hashitani et al. (2001) have indeed been able to demonstrate a punctate connexin-43 immunofluorescence by using confocal microscopy. However, these fluorescence dots are located at the long sides of the cells, making it difficult to explain the observation that the cells are coupled preferentially in the axial direction. Unfortunately, the authors do not include an electron micrograph to illustrate their finding of gap junctions at ultrastructural level and so the exact nature and location of gap junctions or gap-like junctions in native guinea-pig detrusor has still to be elucidated.

To achieve an easier experimental approach to the study of gap junctions, we have cultured smooth muscle cells from guinea-pig bladder. We have chosen fragment cultures, because these mixed culture resemble the in situ conditions more closely than do pure smooth muscle cell cultures. This notion is supported by our observation that the smooth muscle cells in cultures, which are almost devoid of urothelium, do indeed grow more slowly and show less pronounced smooth-muscle-cell-like morphology. By immunocytochemical detection of established smooth muscle cell markers, we have been able positively to identify smooth muscle cells in our cultures as the major component. Cultured colonic smooth muscle cells have been used in dye-coupling experiments to demonstrate propagation between cells by using fura-2 calcium imaging (Young et al. 1996). The colonic smooth muscles show comparable propagation properties of the calcium wave. As described by Young et al. (1996), the calcium elevation is not regenerative, i.e. the signal declines with the distance. This speaks in favour of a diffusible factor being propagated through the gap junctional channels. In contrast to the study of Young et al. (1996), we have not seen "silent" cells that propagate the calcium wave without showing a calcium elevation themselves. In some experiments, we have had this impression but careful phase-contrast-microscopic examination has revealed very thin cytoplasmic protrusions (data not shown) of the distant cell out of the focal plane making contact with the stimulated cell. Thus, we do not think that there is enough evidence for "silent" cells conducting the signal as yet.

As demonstrated by electron microscopy (Fig. 6), cultured smooth muscle cells form multilayers and are interconnected by multiple gap junctions. Dye-coupling has revealed extensive coupling, leading to functional syncytia containing up to 100 cells. This is in clear contrast to the in situ findings, where the syncytia are much smaller. Thus, the cultured smooth muscle cells resemble

a pathological state as defined by the abundance of gap junction formation (Elbadawi et al. 1993), which is greater than in the unaltered detrusor muscle.

Interestingly, the calcium waves initiated by electrical stimulation of single cells rather seldom travel more than two cells from the stimulated cell. This could mean that the calcium wave is conducted by a short-range diffusible factor or alternatively that the gap junctions (which are abundant in these cultures) are quickly closed (within milliseconds).

By Western blotting, we have been able to demonstrate that the major component of the gap junction in situ and in vitro is connexin-43. The reason for the slightly higher molecular weight (56 kDa) of the connexin-43-positive band should be investigated. From these experiments, one would expect many gap junctions to be found in the guinea-pig bladder, since the expression is as high as in guinea-pig heart (Fig. 4). One explanation might be that not all of the connexin-43 protein is arranged in gap junctions that show the classical morphological arrangement of the connexons. This notion is supported by the study of Li et al. (1996) who have provided evidence for the existence of nonjunctional plasma connexin-43 hemichannels in hepatoma cells.

In conclusion, cultured smooth muscle cells from the guinea-pig detrusor are a feasible model system for studying the expression and the physiological characteristics of gap junctions in vitro. Since smooth muscle cells seem to stay in a less differentiated state than in situ and form many more gap junctions, this culture system will be valuable for investigating the regulation of gap junction expression as a pathological relevant feature in vitro. The size and location of gap junctions in situ are still obscure and have to be examined in further studies, including connexin-43 immunocytochemistry at the electron-microscopic level.

Acknowledgements The authors are grateful to Mrs. M. Dettmer, Mrs. A. Weimann, Mr. M. Mewe and Dr. W. Dawood for their technical assistance with cell culture and Ca-imaging. We thank Mrs. R. Knittel for help with electron microscopy and freeze-fracturing.

References

Beyer EC, Paul DL, Goodenough DA (1987) Connexin43: a protein from rat heart homologous to a gap junction protein from liver. J Cell Biol 105:2621–2629

Bradford MM (1976) A rapid and sensitive method for quantification of microgram quantities of protein utilizing principle of protein dye-binding. Anal Biochem 72:248–254

Brading AF (1997) A myogenic basis for the overactive bladder. Urology 50 (Suppl 6A):57–67

Brink PR (1998) Gap junctions in vascular smooth muscle. Acta Physiol Scand 164:349–356

Christ GJ, Spray DC, el-Sabban M, Moore LK, Brink PR (1996) Gap junctions in vascular tissues. Evaluating the role of intercellular communication in the modulation of vasomotor tone. Circ Res 79:631–641

Dorschner W, Stolzenburg J-U, Neuhaus J (2001) Structure and function of the bladder neck. Adv Anat Embryol Cell Biol 159:1–113

Elbadawi A, Yalla SV, Resnick NM (1993) Structural basis of geriatric voiding dysfunction. III. Detrusor overactivity. J Urol 150:1668–1680

Fishman GI, Spray DC, Leinwand LA (1990) Molecular characterization and functional expression of the human cardiac gap junction channel. J Cell Biol 111:589–598

Fry CH, Wu C (1998) The cellular basis of bladder instability. Br J Urol 81:1–8

Fry CH, Cooklin M, Birns J, Mundy AR (1999) Measurement of intercellular electrical coupling in guinea-pig detrusor smooth muscle. J Urol 161:660–664

Gimona M, Herzog M, Vandekerckhove J, Small JV (1990) Smooth muscle specific expression of calponin. FEBS Lett 274:159–162

Grynkiewicz G, Poenie M, Tsien RY (1985) A new generation of calcium indicators with greatly improved fluorescence properties. J Biol Chem 260:3440–3450

Hailemariam S, Elbadawi A, Yalla V, Resnick NM (1997) Structural basis of geriatric voiding dysfunction. V. Standardized protocols for routine ultrastructural study and diagnosis of endoscopic detrusor biopsies. J Urol 157:1783–1801

Hanani M, Brading AF (2000) Electrical couping in smooth muscles. Is it universal? J Basic Clin Physiol Parmacol 11:321–330

Hashitani H, Fukata H, Takano H, Klemm MF, Suzuki H (2001) Origin and propagation of spontaneous excitation in smooth muscle of the guinea-pig urinary bladder. J Physiol (Lond) 530:273–286

Kimura H, Oyamada Y, Ohshika H, Mori M, Oyamada M (1995) Reversible inhibition of gap junctional intercellular communication, synchronous contraction, and synchronism of intracellular Ca^{2+} fluctuation in cultured neonatal rat cardiac myocytes by heptanol. Exp Cell Res 220:348–356

Klöckner U, Isenberg G (1985) Action potentials and net membrane currents of isolated smooth muscle cells (urinary bladder of the guinea-pig). Pflügers Arch 405:329–339

Laemmli UK (1970) Cleavage of structural proteins during the assembly of the head of bacteriophage T4. Nature 227:680–685

Li H, Liu TF, Lazrak A, Peracchia C, Goldberg GS, Lampe PD, Johnson RG (1996) Properties and regulation of gap junctional hemichannels in the plasma membranes of cultured cells. J Cell Biol 134:1019–1030

Little TL, Xia J, Duling BR (1995) Dye tracers define differential endothlial and smooth muscle coupling patterns within the arteriolar wall. Circ Res 76:498–504

Miyoshi H, Boyle MB, MacKay LB, Garfield RE (1996) Voltage-clamp studies of gap junctions between uterine muscle cells during term and preterm labor. Biophys J 71:1324–1334

Neuhaus J, Stolzenburg J-U, Stenzel M, Dorschner W (2000) Alterations of the calcium concentration in cultured smooth muscle cells of the lower urinary tract following pharmacological stimulation. Aktuel Urol 31:41–48

Neuhaus J, Dorschner W, Mondry J, Stolzenburg J-U (2001) Comparative anatomy of the male guinea-pig and human lower urinary tract: histomorphology and three-dimensional reconstruction. Anat Histol Embryol 30:185–192

Takahashi K, Hiwada K, Kokubu T (1988) Vascular smooth muscle calponin. A novel troponin T-like protein. Hypertension 11:620–626

Watts SW, Tsai M-L, Loch-Caruso R, Webb RC (1994) Gap junctional communication and vascular smooth muscle reactivity: use of tetraethylammonium chloride. J Vasc Res 31:307–313

Young SH, Ennes HS, Mayer EA (1996) Propagation of calcium waves between colonic smooth muscle cells in culture. Cell Calcium 20:257–271